International Journal of Nanoelectronics and Materials
Volume 15, No. 3, July 2022 [223-240]

Optically Enhanced N doped ZnO Amorphous Nanostructures grown by Low Cost Ultrasonicated Sol–Gel Route

U. P. S. Gahlaut and Y. C. Goswami*

Nano Research Lab, ITM University Gwalior, MP India 474001

Received 13 November 2021, Revised 26 April 2022, Accepted 27 April 2022

ABSTRACT

N doped ZnO amorphous nanostructures with excellent optical properties were grown by the ultrasonicated sol-gel route. The samples were characterized using structural, morphological and optical studies. XRD patterns confirmed the hexagonal wurtzite structure of ZnO. Increase in nitrogen doping results in effective structural changes like decrease in FWHM of peak (34.30), appearance of additional peaks and removal of previous peaks. The crystallite size of undoped ZnO is calculated at around 5.88 nm and decreases to 3.525 nm, 3.386 nm, and 3.008 nm respectively on gradual increase in nitrogen doping concentration in the samples B: 0.05M, C: 0.1M, and D: 0.2M respectively. The morphological pattern of these nanostructures shows that on increasing the doping of nitrogen, the roughness of the surface increases. An optical study shows that on doping of nitrogen, the bandgap decreases results in absorption shifts in the visible region. Two peaks at 480nm and 685nm are observed due to defects of ZnO surface. The addition of nitrogen generates acceptor levels near the valance band edge. The peak at 450 nm might be due to transition from the conduction band to shallow acceptor levels near the valance band. The presence of a peak near 665 nm indicates the formation of deep holes levels. Significant shift in band edge, the morphological changes and decrease in size indicates successful doping in terms of nitrogen content and homogeneity. Nitrogen doping and metal vacancies stabilize shallow acceptors levels above the valence band in ZnO, thus triggering the stabilization of a p-type conductivity as indicated in luminescence studies.

Keywords: ZnO, Doping, Optoelectronics devices, Semiconductors

1. INTRODUCTION

The research interest in wide bandgap semiconducting materials has been renewed because of their applications in optoelectronic devices [1]. Zinc oxide is one of the most useful candidates for this purpose because of its large exciton binding energy (60MeV) and direct bandgap (3.37eV). Having a wide bandgap makes zinc oxide (ZnO) transparent in the visible region of the electromagnetic spectrum and therefore, makes it useful in various purposes like transparent conducting oxide, shield against high energy radiation, blue/UV solid-state emitters and transparent thin-film transistor and quantum mechanical applications [2-7].

ZnO shows various properties which depend on doping, including the type of doping (n-type or p-type), ultrasonic oscillator [8], chemical sensing [9] and LED [10]. To realize the applications of ZnO in devices, it is necessary to have both n-type and p-type versions of ZnO. Naturally, ZnO is an n-type semiconductor [11], therefore, to make ZnO-based devices it is necessary to investigate the various method of obtaining p-type ZnO. Theoretical investigation shows that shallow acceptors levels can be obtained in ZnO by various doping mechanisms [11-13]. Nitrogen (N) is most suitable for p-type doping because of its atomic size and electronic structure consideration

*Corresponding author: ycgoswami@gmail.com

[14]. Various techniques like MBE, PLD, IBS and magnetron sputtering have been used to grow N-doped ZnO thin films [14-17]. Despite the report of continuous progress over the years, fabrication of a genuine p-doped material is still elusive. N ion can enter in ZnO in two different manners, either substituting the oxygen site (NO) or after making a defect complex in combination with Zn (NO−V Zn) or O vacancies (N Zn−VO) [14,18]. As per the theory, a deep acceptor level is induced by the impurity ions in the ZnO bandgap, which is the reason behind a broad luminescence peak at around 730 nm [19, 20]. Low carrier mobility is one of the hindrances in the use of N-doped samples as p-type semiconducting oxide [21].

In this paper, we proposed a low cost ultrasonicated assisted sol-gel route to grow N-doped ZnO thin films and its structural, optical, and morphological characterizations were analyzed.

2. MATERIAL AND METHODS

2.1 Chemicals

All the chemicals used in the experiment were analytical grade purchased from Ranbaxy India and used without further purification. Zinc chloride (ZnCl2.2H2O) dihydrate was used for Zn element. Ammonium chloride (NH4Cl) was used for nitrogen doping. Ethanol (C2H5OH) and hydrochloric acid (HCl) were used as solvents. Double distilled water was used for solution preparation. The ZnO and their doped samples were prepared in two stages: (1) synthesis of ZnO gel, (2) N doped ZnO nanostructures.

2.2 Synthesis of ZnO Nanostructures

Zinc oxide (ZnO) gel was obtained by modified sol-gel route. In this method, the solution was treated in ultrasonic environment that helps in obtaining uniform particles of small size. 0.05 M zinc chloride as a zinc source is added to the mixture of 40 ml of ethanol and 10 ml of distilled water. About 3ml of hydrochloric acid (HCl) was added in the solution. The solution was agitated ultrasonically for 45 minutes at 60^0C to break up the agglomerates, creating a relatively stable nanosize suspension. Finally, the solution was kept for another 24 hours for aging. A transparent sol was obtained and divided into two parts, one of them was used for the synthesis of undoped ZnO layers on glass substrates and another part was used for development of nitrogen doped ZnO thin films.

2.3 Synthesis of N doped Structures

For obtaining nitrogen doped zinc oxide layers, ammonium chloride (NH4Cl) was used as doping precursor. For doping, various molar ratios (0.05M, 0.1M and 0.2M) of ammonium chloride were used. It has been added into 10ml of ethanol separately and mixed thoroughly using magnetic stirring. Finally, it has been added in as-prepared gel of zinc oxide. The mixture was stirred well for 30 minutes with magnetic stirrer. Ultrasonic vibrations were introduced for about 60 minutes and at 60^0C temperature that helps in uniform distribution. Finally, the solution was aged for another 20 hours before analyzed.

2.4 Characteristics Techniques

The samples were structurally characterized using morphological and optical characterizations. For structural studies, the x ray diffractograms were obtained in the 2θ range from 20^0 to 80^0 with Cu Kα radiation of wavelength 1.546 Å using Bruker D8 Advanced X ray Diffraction unit. Microscopic studies were performed using Atomic Force Microscopy (AFM) make digital Instrumentation—Inc, USA. UV Vis Transmission spectra were obtained using Perkin Elmer Lambda 25 UV VIS Spectrophotometer in the range of 200nm to 800nm. Photoluminescence spectra for undoped and doped ZnO were obtained using Perkin Elmer LS55 fluorescence Spectrophotometer with exciton at 200 nm using Xe lamp.

The N-doped ZnO nanostructures were grown by the ultrasonicated sol-gel route. The synthesized thin films have been labeled as samples A, B, C, and D respectively. Sample A was undoped ZnO and samples B to D were N doped ZnO with different doping of N in the molar ratios (B: 0.05, C: 0.1, and D: 0.2). The samples were characterized using various techniques including structural, photoluminescence, morphological and optical properties, and are discussed below.

2.1 Structural Analysis

Figure 1 shows the X-ray diffraction pattern of undoped N-ZnO nanostructures. Broad peak is observed, indicates the nanostructure formation. Along with broad peak, sharp peaks are also observed. The XRD spectra of undoped ZnO shows the broad peak at 23^0 (111) and sharp peak at 34.65^0 (220) which confirms hexagonal wurtzite zinc oxide structures (JCPDS file 05-0664) [22]. The peaks observed in nitrogen doped samples (samples B-D) 26.50^0, 32.10^0 and 34.30^0, and 36.10^0 are indexed as (100), (002), (220) and (101) respectively. The additional peak is observed at 29.670^0 in sample D having high N-doping. The crystallite size is calculated by the Debye Scherrer formula using full with half maxima of the broad peak [23]. The crystallite size of undoped ZnO is found at around 5.88 nm. In samples B-D, the crystallite size is calculated as 3.525 nm, 3.386 nm, and 3.008 nm respectively. Addition of nitrogen improves the crystallinity and also observance of additional peaks. This ensure that the nitrogen doping affects the structural of ZnO and also results in decrease in size.

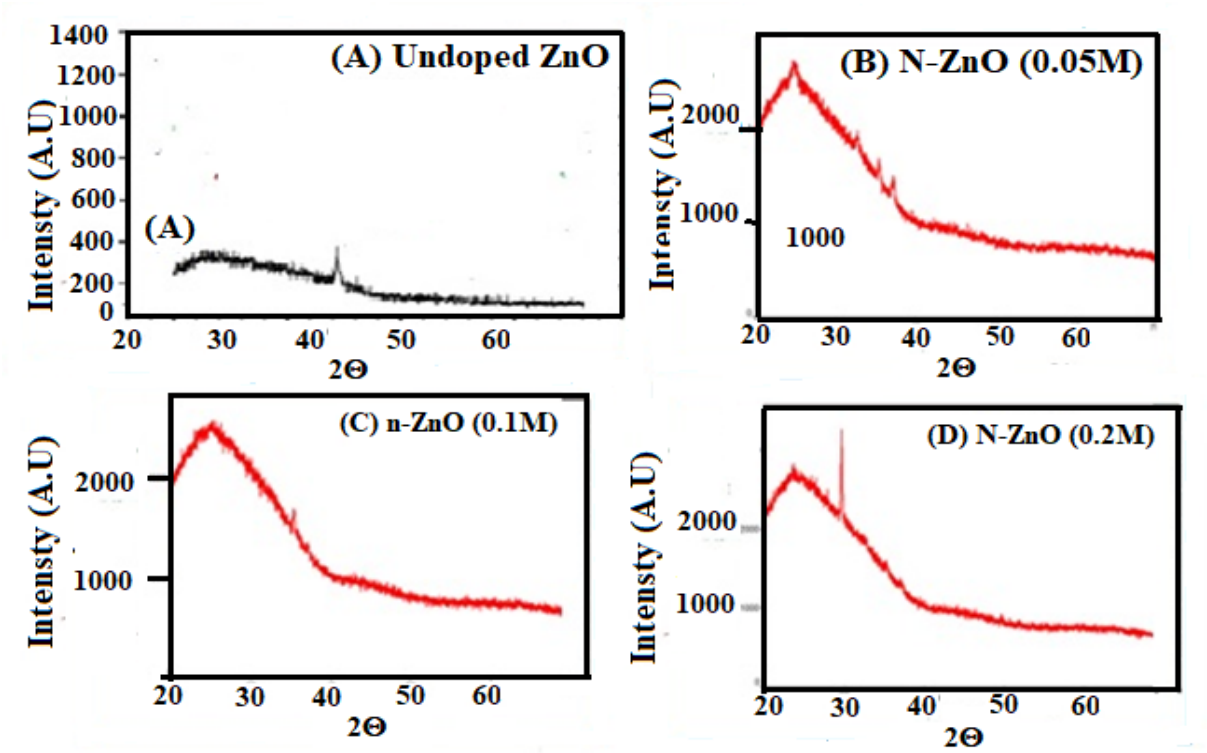

Figure 1. X-ray diffractograms of (B) (C), (D) of N doped ZnO nanostructures**3.2 Morphological Studies**

Figure 2A shows AFM topographic images (2D and 3D) of undoped ZnO and doped ZnO(Figure 2B, 2C, 2D) with increasing concentration of nitrogen (0.05M, 0.1M and 0.2M). The general features of film morphology are the same in both doped and undoped cases, apart from the appearance of pits that becomes bigger in doped film. These pits might be introduced by nitrogen-induced defects during nitrogen exposure and combine into large pits in the subsequent aging step. Nitrogen incorporation leaves morphological fingerprints in the AFM images.

Figure 2A shows homogeneously covered undoped ZnO with Å-sized protrusions due to the OH groups. In the literature, the reason behind these protrusions is OH groups [24]. In the doped ZnO micrographs, very feeble depressions were observed on the surface which grows in numbers on increasing concentration of nitrogen. Since our spatial resolution is finite, we cannot say whether those minima are due to dopants or due to secondary defect which appears during the inclusion of nitrogen. Nitrogen doping introduces a shallow to deep acceptor level (through anionic substitution) that reduces the electron concentration of ZnO.

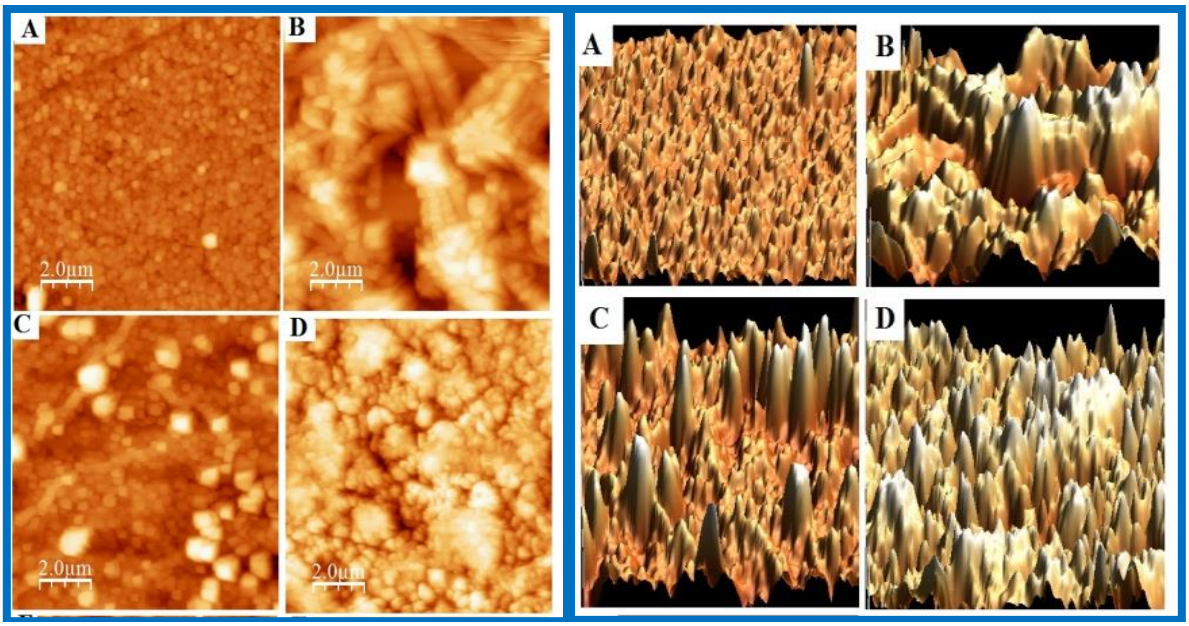

Figure 2. 2-D and 3-D AFM micrographs of (A) undoped ZnO, (B), (C) and (D) N Doped ZnO

3.3 Photoluminescence Studies

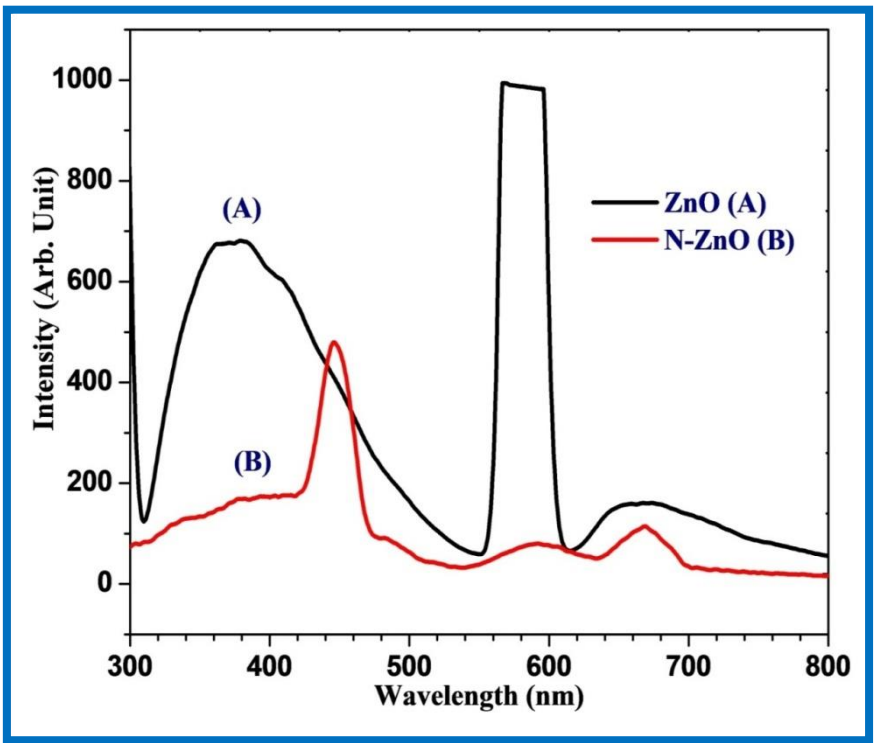

Figure 3. PL spectra of undoped sample (A) ZnO and (B) N doped ZnO heterostructures

Photoluminescence (PL) of undoped ZnO and N doped ZnO (0.2M) nanostructures are shown in Figure 3, where PL spectra gives important information about the charge carrier separation and recombination during excitation. In undoped ZnO, two peaks at 385nm and 580nm are observed. The peak at 385nm lies near the band edge of ZnO. On addition of nitrogen, the peaks observed at 450nm and 680 nm. The peak observed around 580-680 nm generally comes from the defects of ZnO surface [25]. The addition of nitrogen generates deep acceptor levels near the valance band edge.

The peak at 450nm might be due to the transition from the conduction band to shallow acceptor levels near the valance band. The presence of a peak near 665nm indicates the formation of deep holes levels. This show that defects help in effective doping. The enhancement in luminescence at higher wavelength with inclusion of nitrogen is establishing the fact that the zinc oxide, surface and grain boundaries are susceptible to electron trapping and oxygen chemisorption, which results in space-charge region formation. The space charge region formed due to defects, impurities and unsaturated bonds contribute to exhibiting effective luminescence in visible region.
all defects, kinks impurity any unsaturated bonds contribute and such potential in surface attributes to generation in effective luminescence.
All

3.4 Optical Absorption Studies

Optical absorption spectra of undoped ZnO and N doped ZnO are obtained and shown in Figure 4. The undoped ZnO spectrum shows the absorption peak around 240nm. A significant shift in absorption is observed on addition of high doping of nitrogen in sample B. The absorption occurs at 325nm which shows a decrease in bandgap. The value of bandgap found in samples A and B are 3.3 eV and 2.85 eV respectively. Furthermore, the electron mobility in the ZnO:N is lower than in the ZnO, which may be used for improvement in device efficiency due to better transportation through the ZnO:N structures.

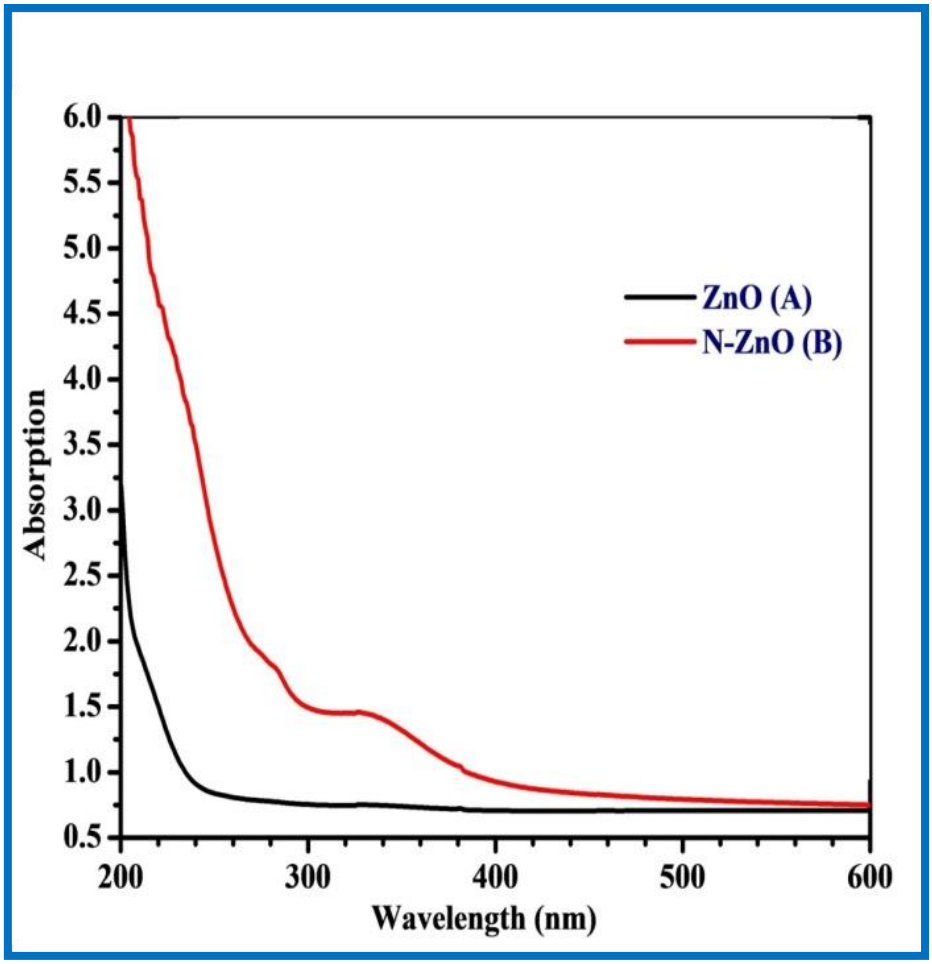

Figure 4. Absorption spectra of undoped ZnO and N doped ZnO heterostructures

3. CONCLUSION

In this work, we have reported synthesis of ZnO and N doped ZnO nanostructures through the ultrasonically assisted sol-gel method. XRD pattern exhibits the characteristic peaks of ZnO which confirms the hexagonal wurtzite structure of ZnO. The morphological pattern of these nanostructures shows that as we increase the doping of nitrogen, the roughness of the surface increases. This fact can be utilized in gas sensing properties. An optical study shows that on doping, the bandgap decreases, therefore the absorption range increases in the visible region. This can be used in optoelectronic devices.

ACKNOWLEDGEMENTS

The authors are thankful to UGC DAE Consortium for scientific research, Indore for providing structural and morphological characterizations, and PC ray research Centre ITM University Gwalior for Optical and PL facilities.

REFERENCES

[1] Z.L. Wang; J. Phys. Vol **16**, (2004) pp.R829.
[2] Ü. Özgür, Y.I. Alivov, C. Liu, A. Teke, M. Reshchikov, S. Doğan, V. Avrutin, S.J. Cho, H. Morkoc; J. Appl. Phys. Vol **98**, (2005) pp.04130.
[3] C. Agashe, O. Kluth, G. Schöpe, H. Siekmann, J. Hüpkes, B. Rech, Thin Solid Films Vol 442, (2003) pp.167–172.
[4] J. Nishii, A. Ohtomo, K. Ohtani, H. Ohno, M. Kawasaki, J. Appl. Phys. Vol **44**, (2005) pp.1193.
[5] S Nagaich, YC Goswami, Fifth International Conference on Advanced Computing & Communication, pp. 165-168, doi: 10.1109/ACCT.2015.16.
[6] R Bisauriya, D Verma, YC Goswami, Journal of Materials Science: Materials in Electronics Vol **29** (3), (2018) pp.1868-1876.
[7] V Kumar, P Rajaram, YC Goswami, Journal of Materials Science: Materials in Electronics Vol **28** (12), (2017) pp. 9024-9031
[8] D.E. Devoe, Sensors Actuators A. Vol **88**, (2001) pp.263.
[9] S.J. Pe167–172,arton, D.P. Norton, K. Ip, Y.W. Heo, T. Steiner, Prog. Mater. Sci. Vol. **50**, (2005) pp. 293.
[10] M.H. Huang, S. Mao, H. Feick, H. Yan, Y. Wu, H. Kind, E. Weber, R. Russo, P. Yang, Science Vol. **292**, (2001) pp. 1897, (2001).
[11] Anderson Janotti and C.G.V.D. Walle, Rep. Prog. Phys. Vol. **72**, (2009) pp. 12650.
[12] UPS Gahlaut, V Kumar, YC Goswami, Physica E: Low-dimensional Systems and Nanostructures Vol **117** (2020) pp. 113792.
[13] UPS Gahlaut, V Kumar, RK Pandey, YC Goswami, Optik Vol **127** (10), (2016) pp. 4292-4295
[14] D.C. Look, D.C. Reynolds, C.W. Litton, R.L. Jone, D.B. Eason and G. Cantwell, Appl. Phys. Lett. Vol. **81**, (2012) pp. 1830.
[15] M. Joseph, H. Tabata, H. Saeki, K. Ueda, T. Kawai, ", Physica B, Vol. **302**, (2001) pp. 140–148.
[16] L.C. Chao, Y.R. Shih, Y.K. Li, J.W. Chen, J.D. Wu, C.H. Ho, Appl. Surf. Sci., Vol. **256** (2010) pp. 4153–4156 (2010).
[17] E. Alves, N. Franco, N. Barradas, F. Munnik, T. Monteiro, M. Peres, J. Wang, R. Martins, E. Fortunato, Vacuum Vol . **83**, (2009) pp. 1274–1278.
[18] Liu, L.; Xu, J.; Wang, D.; Jiang, M.; Wang, S.; Li, B.; Zhang, Z.; Zhao, D.; Shan, C.- X.;Yao, B.; Shen, D. Z., Phys. Rev. Lett. Vol. **108**, (2012) 215501-1–4.
[19] Varley, J. B.; Janotti, A.; Franchini, C.; Van de Walle, C. G. Phys. Rev. B Vol **85** (2012), pp. 081109-1–4.
[20] Lyons, J. L.; Janotti, A.; Van de Walle, C. G. Why nitrogen cannot lead to p-type conductivity in ZnO. Appl. Phys. Lett. 2009, Vol **95**, (2009) pp. 252105-1–3.
[21] Showkat Hassan Mir Vivek Kumar Yadav and Jayant Kumar Singh, *ACS Omega* Vol. **24** Issue 5 (2020) pp. 14203–14211.
[22] UPS Gahlaut, V Kumar, RK Pandey, YC Goswami, Advances in Optical Science and Engineering, Springer Proceedings in Physics, vol **166** https://doi.org/10.1007/978-81-322-2367-2_43.

[23] B.D. Cullity, S.R. Stock, Elements of X-Ray Diffraction, third ed., Prentice-Hall Inc, Canada, (2001) pp. 167–171.
[24] Fernando Stavale, Leandro Pascua, Niklas Nilius, and Hans-Joachim Freund *J. Phys. Chem. C* 2014, 118, 25, 13693–13696
[25] Lauritsen, J. V.; et al.. ACS Nano Vol. **5**, (2011) pp. 5987−5994.